Well-confined surface plasmon polaritons for sensing applications in the near infrared

Choon How Gan, Philippe Lalanne

Well-confined surface plasmon polaritons for sensing applications in the near-infrared

C. H. Gan* and P. Lalanne

Laboratoire Charles Fabry de l'Institut d'Optique, CNRS, Univ Paris-Sud, Campus Polytechnique, 91127 Palaiseau cedex, France

**Corresponding author: choon.gan@institutoptique.fr*

Received November 30, 2009; revised January 13, 2010; accepted January 14, 2010; posted January 20, 2010 (Doc. ID 120602); published February 12, 2010

The surface plasmon polariton (SPP) dispersion at the interface between a dielectric half-space and a layered metallodielectric metamaterial is investigated. By varying the material constituants, it is shown that the SPP resonance frequency can be readily shifted to the near-IR. Through numerical simulations, the validity domain of homogenization and the effects of the finite number of layers in the metamaterial are studied. It is found that as few as $N=2$ periods are sufficient for practical operation. These results reveal the potential of employing metallodielectric stacks for sensing applications in the near-IR regime. © 2010 Optical Society of America

OCIS codes: 260.1960, 240.6680.

Light confinement plays an important role in many optical applications. For instance, it limits the minimum lateral size of waveguides in integrated optoelectronics and the achievable resolution of various optical imaging systems. The culprit behind these limitations is the diffraction limit, which prevents confinement of light waves to dimensions smaller than about half its wavelength in the medium. Recently, SPPs, whose wavenumbers are larger than those of light photons at a given energy [1], have been employed for applications such as subwavelength photolithography [2], imaging [3], biosensing [4,5], and light confinement in optical waveguides [5,6]. At a bulk metal–dielectric interface, the SPP disperison relation is given by $k_{x0}=k_0\sqrt{\varepsilon_1\varepsilon_m/(\varepsilon_1+\varepsilon_m)}$, where $k_0=\omega/c$ is the wavenumber in free space and ε_1 and $\varepsilon_m=\varepsilon_m'+i\varepsilon_m''$ are the dielectric constants of the dielectric and metal. The SPP resonance occurs at the frequency ω_{sp} for which the real part of the denominator of k_{x0} vanishes. Assuming a Drude model ($\varepsilon_m'=\varepsilon_\infty-\omega_p^2/\omega^2$) for the permittivity of the metal, one finds that $\omega_{sp}=\omega_p/\sqrt{\varepsilon_1+\varepsilon_\infty}$, where ω_p is the bulk plasma frequency and ε_∞ is the high frequency dielectric constant of the metal. Because ω_p is usually in the UV for noble metals, ω_{sp} typically lies in the deep blue or visible spectrum.

In this Letter, we propose to replace the metal with a metamaterial consisting of N periods of metallodielectric layers, as shown in Fig. 1(a). The SPP resonance of the artificial material can be tuned to near-IR wavelengths, allowing us to synthesize surface modes in this spectral range with confinements similar to those of classical SPPs at visible frequencies. By analogy, we will refer to these surface modes as SPPs. It is worth noting that corrugated metallic films (with nanorods or nanoholes), instead of multilayered structures considered here, have also been shown to support tunable SPP-like modes [4,7,8].

To intuitively understand the impact the alternate layers have on the confinement of the SPP, we start with a simple model using the zeroth-order effective medium theory (EMT) [9]. This allows us to treat the 2-D metamaterial effectively as an anisotropic medium with $\varepsilon_{xx}=(1-f)\varepsilon_d+f\varepsilon_m$ and $1/\varepsilon_{zz}=1-f/\varepsilon_d+f/\varepsilon_m$. Here the fill factor $f=t_m/a$, with t_m being the thickness of the metal layer and a being the period of the multilayered structure. In the near-IR, $|\varepsilon_m|$ is usually large so that ε_{zz} is dielectriclike, and ε_{xx} corresponds to a highly conductive metal, except if f is kept small. As such, only small f values will be considered in the following analysis. The SPP dispersion for the metamaterial–dielectric system may be derived from Maxwell equations as (see, for instance, [6])

$$k_x=k_0\sqrt{\varepsilon_1\varepsilon_{zz}(\varepsilon_1-\varepsilon_{xx})/(\varepsilon_1^2-\varepsilon_{xx}\varepsilon_{zz})}. \quad (1)$$

The SPP resonance of the metamaterial–dielectric interface is obtained for $\mathrm{Re}(\varepsilon_1^2-\varepsilon_{xx}\varepsilon_{zz})=0$, which for the case $f\ll 1$ reduces to the condition

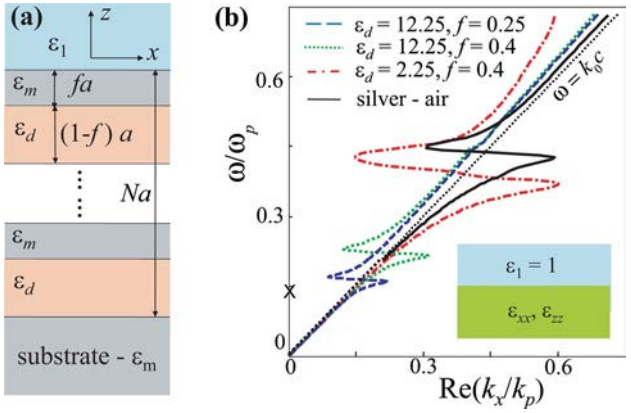

Fig. 1. (Color online) SPP mode at the interface between a metallodielectric metamaterial and a dielectric half-space. (a) Illustration of the proposed geometry. (b) Dispersion relation for the SPP derived using zeroth-order EMT for different values of ε_d and f. The simulated geometry is shown in the inset. The X on the vertical axis indicates where ω/ω_p corresponds to $\lambda=1$ μm.

$$\eta\varepsilon_d|\varepsilon_m'| = \varepsilon_d^2 - \varepsilon_1^2, \tag{2}$$

with $\eta = f/(1-f)$. To calculate the effective SPP resonance frequency $\omega_{sp}^{(eff)}$, we substitute the Drude model for ε_m' in Eq. (2). This yields

$$\omega_{sp}^{(eff)} = \omega_{sp}\sqrt{\eta\varepsilon_d(\varepsilon_1+\varepsilon_\infty)/(\varepsilon_d^2-\varepsilon_1^2)}, \tag{3}$$

which holds for small f and is independent of the fitted value of ε_∞. By comparing with numerical results obtained using a transfer matrix approach [10], it is found that the relative accuracy of Eq. (3) is better than 15% in its domain of validity. For large dielectric permittivity ($\varepsilon_d^2 \gg \varepsilon_1^2$), such as those of semiconductors at telecommunication and near-IR freqencies, Eq. (3) reduces to $\omega_{sp}^{(eff)} = \omega_{sp}\sqrt{\eta(\varepsilon_1+\varepsilon_\infty)/\varepsilon_d}$, showing that the SPP resonance frequency can be artificially decreased by using thin metallic films, or to a lesser extent, by using dielectric layers with a high index of refraction [11]. The dispersion relation of Eq. (1) for an air interface ($\varepsilon_1 = 1$) and for different values of ε_d and f is plotted in Fig. 1(b). In the simulations, the metal in the layered structure is taken to be silver, and its refractive index follows the data of Palik [12]. By fitting the real part of the refractive indices to the Drude model, it is found that the value of the bulk plasmon frequency $\omega_p = k_p/c$ corresponds to a wavelength $\lambda_p \sim 150$ nm, and $\varepsilon_\infty \sim 4$. The wavelength at the SPP resonance for the bulk silver–air interface is approximately 215 nm ($\omega_{sp} = \omega_p/\sqrt{5}$). With $\varepsilon_d = 12.25$ and $f = 0.25$ (blue dashed curve), the SPP resonance wavelength is increased by about four times, close to $\lambda = 1$ μm [$\omega \simeq 0.15\omega_p$ in Fig. 1(b)]. To compare the confinement of the SPP, we note that with the metamaterial instead of the metal, $k_{z1} \approx k_0\varepsilon_1/\sqrt{(f\varepsilon_m)}$, and therefore the decay length (normalized by wavelength) $\delta/\lambda \propto \sqrt{f\varepsilon_m}$. Thus the confinement improves roughly by a factor of $\sqrt{f}$ compared with the case of the bulk silver–air interface, where $\delta/\lambda \propto \sqrt{\varepsilon_m}$ [1]. However, the improved confinement is achieved at the expense of the (normalized) SPP propagation length, given by $L/\lambda = [4\pi\,\mathrm{Im}(n_{spp})]^{-1}$, where $n_{spp} = k_x/k_0$ is the effective index of the SPP. This trade-off between the confinement and propagation loss is typically encountered in the operation of plasmonic devices and will be discussed later on.

The EMT-based analysis above shows that one may push the SPP resonance wavelength ($\lambda_{sp}^{(eff)} = 2\pi c/\omega_{sp}^{(eff)}$) to long wavelengths by using very thin metal films. However, there are some restrictions in practice. First, the metal film thickness t_m should be larger than some threshold value t_p, under which the film is no longer percolated and is formed by islands. For silver or gold, $t_p \simeq 6-10$ nm, depending on the method and temperature of growth [13,14]. Second, to keep the EMT predictions reasonably accurate, the ratio a/λ should remain below some threshold value ζ. Combining these two restrictions, $t_m > t_p$ and $a/\lambda < \zeta$, we get $f\lambda\zeta > t_m$, and by substituting into Eq. (3) we find that $\lambda_{sp}^{(eff)} \lesssim \lambda_p^2\varepsilon_d\zeta/t_m$. As an example, taking $t_m = 8$ nm and $\zeta = 0.1$ [15,16], $\lambda_{sp}^{(eff)} \sim 3.5$ μm, implying that $\lambda_{sp}^{(eff)}$ is not readily extendable to thermal IR wavelengths.

Working toward a practical device, it is important to analyze the effects of the finite period a and of the number of periods N, since the thickness of the metamaterial stack is necessarily finite. For a quantitative assessment, we have performed fully vectorial calculations using the transfer matrix approach. We first consider an infinitely layered metamaterial ($N \to \infty$) and look at the effects of the finite period. For the sake of illustration, let us consider operation at telecommunication wavelengths, namely, $\lambda_1 \simeq 1.55$ μm. Using $\lambda_{sp}^{(eff,1)} = 1$ μm as the target resonance wavelength, one finds from Eq. (3) that $f = 0.21$. For $t_m = 8$ nm, the associated period is $a = 38$ nm. The deviations between the EMT predictions and fully vectorial calculations are shown in Fig. 2(a), where $\mathrm{Re}(n_{spp})$ is plotted as a function of wavelength for $f = 0.21$. We also consider the case when t_m is doubled to 16 nm ($a = 76$ nm), which is relatively more conducive for fabrication. As expected, the deviations from the EMT predictions escalate as the period a increases, and smaller values of $\mathrm{Re}(n_{spp})$ are obtained. Note that smaller $\mathrm{Re}(n_{spp})$ values correspond to longer effective wavelengths for the SPP and therefore to worse confined modes. This can be understood physically, because an optically thick metal layer (with thickness greater than the skin depth) behaves like a bulk metal. The normalized confinement δ/λ and propagation length L/λ for the case $f = 0.21$ ($a = 38$ nm) are shown in the top panel of Fig. 2(b). At $\lambda_1 \simeq 1.55$ μm, $\delta/\lambda \simeq 0.34$ for the SPP mode of the metamaterial–air interface (red dashed curve), which is less than half of that of the bulk silver–air interface (red solid curve). This better confinement is attained with a compromise in the normalized propagation length, which is reduced to

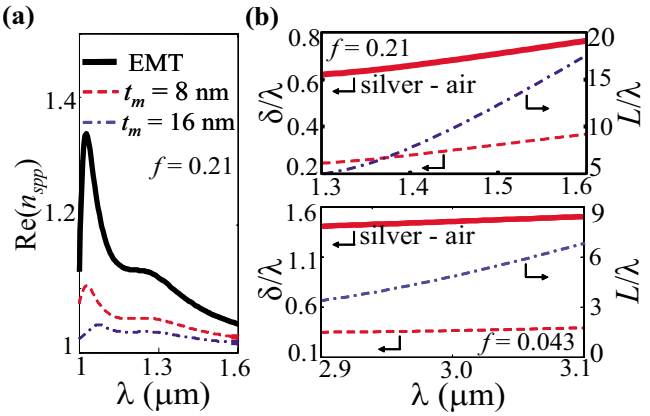

Fig. 2. (Color online) Characteristics of an SPP designed to have a strong confinement at $\lambda_1 = 1.55$ μm ($f = 0.21$) and $\lambda_2 = 3$ μm ($f = 0.043$). (a) Comparison between EMT predictions (black solid curve) and fully vectorial calculations for $t_m = 8$ nm (red dashed curve) and 16 nm (blue dashed-dotted curve), for $f = 0.21$. (b) Normalized confinement (δ/λ) and propagation length (L/λ) for $f = 0.21$ (top) and $f = 0.043$ (bottom), calculated with $t_m = 8$ nm. The red solid curves show the normalized confinement for a silver–air interface.

$L/\lambda \simeq 15$. Similar trends are observed for the metamaterial–air interface supporting a confined SPP mode at near-IR wavelengths ($\lambda_2 \simeq 3$ μm, $\lambda_{sp}^{(eff,2)} = 2.5$ μm). As seen from the bottom panel of Fig. 2(b) for this latter case ($f = 0.043$, $a = 184$ nm), we find $\delta/\lambda_2 \simeq 0.37$, $\simeq 25\%$ that of the silver–air interface, and $L/\lambda_2 \simeq 5.5$.

We now turn to the question of the number of periods N required for a device. Naively, one might think that a large N is necessary. Actually this is not the case, because the SPP mode at the metamaterial–air interface is greatly attenuated over a single period. It turns out that as few as $N = 2$ periods could suffice, which considerably reduces the fabrication complexity. To illustrate our purpose, let us consider the structure with $\lambda_{sp}^{(eff,1)} = 1$ μm and $t_m = 8$ nm as before and examine the confinement and propagation distance of the SPP as a function of N at an operating wavelength $\lambda_1 = 1.55$ μm. The thickness of the substrate should exceed a few times the skin depth to render it optically opaque. The results are shown in Fig. 3. Remarkably, one finds that δ/λ for the case $N = 2$ is only about 10% larger than that obtained for $N \to \infty$. The associated SPP mode profile is shown in the inset. In this case, the metamaterial with $N = 2$ periods offers at 1.55 μm, a level of confinement that corresponds to that of the classical SPP mode at a silver–air interface at a wavelength of 750 nm. Computational results for the structure with $\lambda_{sp}^{(eff,2)} = 2.5$ μm and $t_m = 8$ nm have shown that a similar confinement can also be achieved at $\lambda_2 = 3$ μm with $N = 2$ periods.

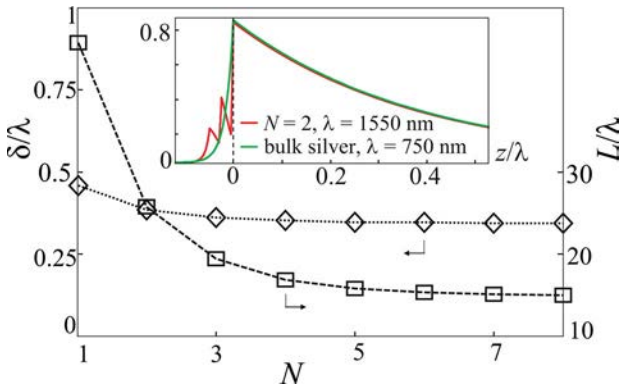

Fig. 3. (Color online) Effects of finite N on the confinement (δ/λ) and the propagation length (L/λ) for $\lambda = 1.55$ μm, $t_m = 8$ nm, and $a = 38$ nm. In the inset, the SPP mode profile ($|H_y|^2$) is shown for the case $N = 2$, and is compared to that at a bulk silver–air interface at $\lambda = 750$ nm [light gray curve (green online)]. The position of the interface is indicated by the vertical dashed line.

For $N = 2$, one could arguably have the flexibility to optimize the structure for two slightly different periods, i.e., $a_1 \neq a_2$, where $a_1 = t_{m1}/f_1$ and $a_2 = t_{m2}/f_2$. Our calculation shows that the SPP behavior is dominated by the upper layer closest to the dielectric half-space. This is because the SPP fields are most intense at the interface. For the case $t_{m2} < t_{m1}$, δ/λ decreases, the confinement improves, but the propagation loss L/λ increases and vice versa. Therefore, for a given t_{m1}, the designer can fine tune the response of the metamaterial by varying the thickness of the metallic film in the bottom layer.

In conclusion, we have demonstrated that surface modes at near-IR wavelengths with a confinement similar to those of classical SPPs in the visible regime exist at the interface between a layered metallodielectric metamaterial and a dielectric half-space. We believe that similar conclusions could be reached for other kinds of surface modes, such as the long- or short-range SPP modes in thin metal films [1].

J. P. Hugonin is acknowledged for computational assistance. C. H. Gan acknowledges a fellowship award from A*STAR of Singapore.

References

1. H. Raether, *Surface Plasmons on Smooth and Rough Surfaces and on Gratings* (Springer, 1988).
2. X. Luo, and T. Ishihara, Opt. Express **12**, 3055 (2004).
3. B. Wood, J. B. Pendry, and D. P. Tsai, Phys. Rev. B **74**, 115116 (2006).
4. A. V. Kabashin, E. Pevans, S. Pastkovsky, W. Hendren, G. A. Wurtz, R. Atkinson, R. Pollard, V. A. Podolskiy, and A. V. Zayats, Nature Mater. **8**, 867 (2009).
5. S. Lal, S. Link, and N. Halas, Nat. Photonics **1**, 641 (2007).
6. J. Elser, A. A. Govyadinov, I. Avrutsky, I. Salakhutdinov, and V. A. Podolskiy, J. Nanomater. **2007**, 79469 (2007).
7. J. B. Pendry, L. Martín-Moreno L, and F. J. Garcia-Vidal, Science **305**, 847 (2004).
8. Z. Shi, G. Piredda, A. C. Liapis, M. A. Nelson, L. Novotny, and R. W. Boyd, Opt. Lett. **34**, 3535 (2009).
9. M. Born and E. Wolf, *Principles of Optics*, 7th ed. (Cambridge U. Press, 1999).
10. A. Yariv, and P. Yeh *Optical Waves in Crystals* (Wiley-Interscience, 2003).
11. J. T. Shen, P. B. Catrysse, and S. Fan, Phys. Rev. Lett. **94**, 197401 (2005).
12. E. D. Palik, *Handbook of Optical Constants of Solids* (Academic, 1985).
13. B. Gergen, H. Nienhaus, W. H. Weinberg, and E. M. McFarland, J. Vac. Sci. Technol. B **18**, 2401 (2000).
14. B. Gompf, J. Beister, T. Brandt, J. Pflaum, and M. Dressel, Opt. Lett. **32**, 1578 (2007).
15. P. Lalanne, and D. Lemercier-Lalanne, J. Opt. Soc. Am. A **14**, 450 (1997).
16. C. Gu, and P. Yeh, Opt. Lett. **21**, 504 (1996).